SHIPBOARD HFDF SYSTEM SIMULATION

Jeffrey B. Knorr
Department of Electrical and Computer Engineering
Naval Postgraduate School
Monterey, CA 93943

Abstract - NEC 4.1 has been used to compute the responses of the antennas in a shipboard high frequency direction finding system which employs the CIDF algorithm to derive bearing estimates. This paper discusses the computational results as well as the performance of the simulation in which the results were utilized.

1. INTRODUCTION

1.1. Background

The requirement to carry out high frequency direction finding (HFDF) from both shore stations and ships arose during WWII. As recounted by Price [1] and Redgment [2], [3], it provided a means for countering the German submarine threat to allied merchant ship convoys. The anti-submarine mission, as well as other modern day missions, continue to make shipboard HFDF an important consideration in the design of electromagnetic systems for many ships.

Direction finding from a ship at high frequencies (HF) is a challenging problem because in the HF band, antennas may interact strongly with the ship's superstructure and their in-situ phase and amplitude responses can deviate significantly from their free space responses. The bearing errors observed using simple systems can be 10°-20° and in some cases, error curves may even be multivalued or discontinuous, as reported by Crampton et al. [4], and Travers et al. [5]. As a result, direction finding (DF) techniques which can be utilized at higher frequencies do not work well aboard ship at HF. At HF, one must use a technique which accounts for the interaction of the antennas with the ship's superstructure. One approach to shipboard HFDF is to use the correlation interferometry direction finding (CIDF) algorithm described by Saucier and Struckman [6]. This algorithm will yield accurate bearing estimates if a sufficiently robust array is used. The algorithm is used to compute the correlation between the complex antenna voltages for an incoming plane wave, and the complex antenna voltages stored in a data base for discrete azimuth angles at the same frequency. The angle of maximum correlation is used as the bearing estimate.

Implementation of a CIDF system aboard ship requires that the ship be calibrated to create the required database of complex receive antenna voltages for frequencies over the range of interest. This is not a problem as a ship can be calibrated after a DF system is installed. Ships, however, are often reconfigured as new systems are added and old systems are removed or upgraded. The effect of associated topside modifications on the complex receive antenna voltages is generally unknown. If the voltages are perturbed, however, DF system accuracy will be degraded. The problem, is that one does not know if topside modifications will cause unacceptable bearing errors.

1.2 Problem

At present, there is no quantitative method for predicting the effect of topside reconfiguration on the bearing accuracy of a shipboard high frequency direction finding system utilizing the CIDF algorithm. One can recalibrate with each reconfiguration, but this is time consuming, expensive, and wasteful of ship operating time. The objective of the work described here was to determine if state-of-the-art hardware and software would support development of a computer based recalibration decision support system.

In general, one is interested in both HF groundwave and skywave signals, and therefore signals which may be elliptically polarized. However, when HF signals are transmitted from ships and submarines at sea, vertically polarized groundwaves can produce useful signal levels at large distances. To simplify the problem, the scope of this initial investigation was therefore limited to

vertically polarized ground waves.

1.3 Approach

A simulation of a high frequency CIDF system was constructed using real ship CIDF software to maintain high fidelity. This software was modified to produce output files containing correlation and bearing estimate values for signals tested against the database. The required calibration database was created by computing the responses of the antennas in the DF array using the Numerical Electromagnetics Code (NEC), version 4.1 [7]. Wire grid models of DD963 Spruance Class destroyers with two different topside configurations were constructed for use with NEC. One ship model had an Anti-Submarine Rocket (ASROC) Launcher in front of the deckhouse, and the other was one where the ASROC launcher was removed and replaced with a Vertical Launch System (VLS). The ASROC launcher was a large rectangular box which was elevated above the deck, whereas the VLS was recessed into the deck and had a much lower profile. These two configurations represented a situation for which the change would raise the recalibration question; a question which at present, cannot be satisfactorily answered. In order to interpret the large correlation and bearing estimate data sets, several programs were written to create 2 and 3-dimensional interactive displays of correlation and bearing error on a Silicon Graphics workstation.

NEC 4.1 was run on both a Silicon Graphics Power Onyx workstation and a CRAY J90 mini supercomputer with 4 processors and 128 MWords (1 GB) of memory. Input and output files were moved over the School's network between these machines and the Silicon Graphics workstation on which the DF system simulation was implemented.

Validation was an important aspect of the work described here. Data for validation were collected in a measurement program in which 1/48th scale brass models of the DD963 were used to measure the amplitude and phase responses of each antenna in the direction finding array. Data were collected for both the ASROC and VLS configurations at 20 frequencies over the range 88.8-1172.64 MHz (1.85-24.43 MHz scaled by the factor 48). Data were also collected for a single DF antenna mounted on a metal box.

The outdoor measurement facility at which the experimental data were collected was located in San Diego, CA. The 11 foot (3.35 meter) long DD963 models were placed on a lead (σ=5x10^6 S/m) turntable and illuminated using a log periodic transmit antenna. This antenna was located at a distance of 79 feet (24.08 meters) from the center of the turntable and was mounted on an arch which permitted the elevation angle to be varied. A signal source and a vector receiver were located in a control room adjacent to the turntable. A sample of the signal from the source was fed to the receiver for use as a phase reference. Amplitude measurements were referenced to a $\lambda/4$ monopole which was used for calibration prior to recording data. Data were collected in 1° steps over the 360° azimuth range.

2. Computation of DF Antenna Responses

The antennas used in the DF array on the 1/48th scale brass model of the DD963 were semi-loops with a 230 mil (0.584 cm.) radius. These were constructed from 0.085 inch (0.216 cm), outside diameter, semi-rigid coaxial cable. The feed was a 15 mil (.38 mm.) slit cut in the outer conductor of the coax at the center of the semi-loop (highest point above the mounting plate). At one end of the semi-loop, the coax was shorted to the mounting plate, and at the other end, the coax passed through the mounting plate to provide an output line.

Accurate computation of the responses of the antennas in the DF array was the most critical element of the work described here. Before computing the response of many antennas arrayed on a ship, the response of a single antenna mounted on a metal box, situated on a ground plane, was investigated.

2.1 Response of a Semi-loop Antenna on a Metal Box

A single semi-loop antenna was mounted on one face of a metal cube, midway between its sides and 8 inches above a ground plane. The metal cube was one foot on a side and the semi-loop was contained in a vertical plane normal

to the face of the box on which it was mounted. The semi-loop was therefore responsive to theta polarized signals, which includes the case of vertically polarized ground waves which were of interest in this study. A wire grid computer model of the structure is shown in Fig. 1, where it can be seen that the semi-loop was modeled numerically using 5 segments (the center segment, #3, is the feed). Measurements and computations were carried out over the scaled frequency range 96-1440 MHz (2-30 MHz unscaled) and the numerical and experimental data were compared. In each case, the excitation was a theta polarized plane wave, incident at an elevation angle of 10 degrees. Fig. 2 shows the amplitude and phase response at 96 MHz where results obtained using NEC are seen to be in good agreement with experimental results. Note that the pattern amplitude is plotted in dB on a relative scale (maximum response = 0 dB). Also shown, are numerical results obtained using the code PATCH [8]. It should be noted that measurements and computations were made for a range of elevation angles with good agreement observed in all cases. A more detailed discussion of this structure, and the results obtained appears in Ref. [9]. Obtaining successful numerical results for a single semi-loop mounted on a box gave confidence that the response of the same antenna could be successfully computed when located on a ship.

2.2 Responses of the Semi-loop Antennas in the Shipboard DF Array

The amplitude and phase responses of semi-loop antennas in a shipboard DF array were computed at four frequencies, 1.85, 6.34, 9.25, and 20.075 MHz, and compared with measurement data at the scaled values of these frequencies (88.80, 304.32, 444.00, 963.60 MHz). Again, the excitation was a theta polarized plane wave, but for the ship, the elevation angle was set at 5 degrees. An elevation angle of 0 degrees could not be used for measurements because the measurement range employed a log periodic dipole array which was mounted on an arch and it could not be lowered into the ground. ASROC and VLS configurations of the DD963 with identical 24 element DF arrays were studied. The DF antennas were deployed around the periphery of the ship, some on the edge of the deck, and some on bulkheads, in approximately mirror image port and starboard locations. Fig. 3a shows a visualization of the numerical model (ASROC configuration), and Fig. 3b shows the 1/48th scale brass model (VLS configuration).

The numerical models of the DD963 consisted of approximately 4000 wires and 7000 segments. Maximum segment length was 1 meter, or 0.1λ at 30 MHz. Some areas of the ship were meshed using a 1 m^2 grid while other areas such as the sides of the ship, were represented using vertical wires spaced by 1 meter. This was considered acceptable since interest here was focused on vertically polarized signals incident over the surface of the sea. For convenience, and to minimize the number of segments in the numerical model, the DF antennas were modeled as 1 m^2 loops in exactly the same locations as the semi-loop antennas in the DF array on the 1/48th scale brass model. The outboard segment of each loop was used as the feed. Although the scaled area of the square loops was about 4 times greater than the area of the semi-loops, both were electrically small, so the difference was of no consequence. There were several areas along the sides of the ship (Fig. 3a) between the deck and the waterline, however, where there were openings as large as 15 meters. As will be shown later, these areas appear to have caused error in the numerical results at the higher frequencies.

Numerical and experimental values of amplitude and phase were generated for each of the 24 antennas in the DF array at the four frequencies mentioned earlier. This resulted in far more data than can be presented here, so only representative results will be shown. The discussion which follows refers to specific antennas in the DF array. The antennas are numbered 1 through 12 going from bow to stern and are designated as port (P) or starboard (S).

To facilitate comparison of data, the results have been displayed for port and starboard antenna pairs, with results for both ASROC and VLS configurations shown on the same plot.

Pattern amplitudes have been normalized (maximum response = 0 dB) to make it easier to compare differences between the configurations. The phase reference is arbitrary both numerically and experimentally, and no attempt was made to match the references. The numerical model of the DD963 is oriented along the x axis in a polar spherical coordinate system. Azimuth is determined by the angle ϕ, which is measured in the x-y plane, in the counter-clockwise direction from the x axis, in accordance with mathematical convention. For measured data, angle is measured clockwise from the bow in accordance with nautical convention. In each case, however, 0 degrees corresponds to the bow of the ship, and the antenna patterns relative to the bow of the ship are correctly depicted, with the port antenna on the left and the starboard antenna on the right. Thus numerical and experimental patterns can be easily compared and their spatial responses are correctly depicted. In the following discussion, the term "azimuth" means relative azimuth in the nautical sense.

Antennas P-3 and S-3 are located on the front of the deckhouse, just behind the ASROC launcher (Fig. 3a). Since these antennas are closest to the ASROC launcher, it was anticipated that they would be most affected by its removal. The surfaces on which these two antennas are mounted are angled outboard by about 20 degrees. Thus, these antennas "look" 20 degrees to port and starboard of the bow, respectively.

Figs. 4a and 4b show the numerical and experimental patterns for antennas P-3 and S-3 at 1.85 MHz. Results for the ASROC configuration appear as a solid curve and results for the VLS configuration appear as a dashed curve. Because the curves are reproduced here in black and white rather than color, the two patterns are indistinguishable in some cases. In this case, the patterns for the two configurations are the same, indicating that the removal of the ASROC launcher had little affect on the patterns of these antennas at this frequency. Both numerical and experimental results show the patterns are approximately omnidirectional with a maximum response about 20 degrees off the bow. The agreement is quite good.

Figs. 5a and 5b show the numerical and experimental phases for antennas P-3 and S-3 at 1.85 MHz. Again, there is essentially no difference between the results for the ASROC and VLS configurations. Phase is plotted within a 360 degree range, so where phase switching occurs, one must visualize an $n2\pi$ (n=integer) translation which would create a continuous curve. Also, when comparing numerical and experimental results, the fact that the phase references are arbitrary, and different, must be taken into account. Thus, numerical and experimental curves must be overlaid and shifted vertically to achieve alignment so they can be compared. This can be done easily at low frequencies, as in the case of Figs. 5, but visual comparison is difficult at higher frequencies where phase varies rapidly and there are many 360 degree discontinuities.

The numerical and experimental phase responses shown in Figs. 5a and 5b are in reasonable agreement. Numerically, the total phase variation is about 175 degrees. Experimentally, it is about 135 degrees. Most of the phase change which occurs for a DF antenna is due to the offset of the antenna from the center of rotation, which is the center of the ship. Experimentally, for example, when the ship is rotated on the turntable, a given DF antenna will move toward or away from the source as the ship rotates. This will cause phase to advance or retard relative to a reference of fixed phase. Antennas P-3 and S-3, for example, are located a full scale distance of 39.56 meters from the center of rotation. Thus, the distance of these antennas from the source changes by 79.1 meters or 0.49λ at 1.85 MHz. This change in position corresponds to a phase change of 175 degrees, which is in good agreement with the numerical result.

The experimental results for P-3 and S-3 are offset from one another by 180 degrees. The phase curve for P-3 starts at about 155 degrees, while that for S-3 starts at about 335 degrees. These results indicate that on the brass model, antenna P-3 was mounted upside down (rotated 180

degrees) with respect to S-3. This is interesting, but has no effect on the correlation and bearing error results presented later. It would have an impact, however, if numerical and experimental results were cross-correlated.

Figs. 6a and 6b show the numerical and experimental patterns for DF antennas P-3 and S-3 at 9.25 MHz. At this frequency, the numerical results show the port antenna looking about 20 degrees to starboard and the starboard antenna looking about 15 degrees to port (the ship is not symmetric about the keel). The experimental patterns show some scalloping in these directions and maxima to either side. The numerical patterns show a lower response in the stern sector than the experimental patterns. The experimental results show more difference between the ASROC and VLS configurations. The agreement between numerical and experimental results at this frequency is still reasonable, although less satisfying than at 1.85 MHz, probably due to deterioriating fidelity of the numerical model.

As a last example, Figs. 7a and 7b show the patterns of DF antennas P-12 and S-12 at 20.075 MHz. These antennas are mounted on the stern, looking aft. At this frequency, the numerical and experimental patterns for some antennas are still in reasonable agreement, but for others there is significant error. For P-12 and S-12, the experimental results show a maximum response at 180 degrees relative azimuth, as one would expect, and response in the bow sector is down 15-30 dB. The numerical results are quite inaccurate for these antennas. The reason for this, it is suspected, is that the several large openings in the side of the hull ($d=\lambda$; see Fig. 3a) resulted in excitation of a field inside the hull at 20.075 MHz.

It is not possible to present all of the numerical and experimental data which were generated in the course of this study, but those data which have been presented above are representative. Related results can be found in Ref. [10]. The conclusion reached, based on inspection of all numerical and experimental results, is that the numerical models of the DD963 produce good results up to about 9 MHz, but need improvement for use at higher frequencies. The addition of vertical wires to close the openings in the sides of the hull would probably result in significant improvement and will be investigated.

3. Correlation and Bearing Error

Numerical and experimental DF antenna amplitude and phase data were used in the computer simulation of the DD963 DF system to study the impact of topside configuration changes on system performance. As mentioned earlier, the specific configuration change examined in the work described here was the removal of an ASROC launcher (located just in front of the deckhouse) and its replacement with a VLS.

The DF antenna responses (amplitude and phase vs. azimuth) for the ASROC configuration constitute a database for that configuration. The DF antenna responses for the VLS configuration constitute a database for that configuration, and also represent the responses which would be measured if a signal were incident on the ship in that configuration. Thus, if a signal vector (the set of complex DF antenna responses for a given azimuth) for the VLS configuration is cross-correlated with signal vectors for the ASROC configuration over all azimuths, the result is a cross correlation curve, the peak of which may be used to derive an estimate of the signal angle of arrival. This procedure simulates the effect of calibrating the ship in the ASROC configuration, then changing configuration to VLS, and using the ASROC database to DF signals received in the VLS configuration.

Numerical and experimental DF antenna response data were used to create databases for the ASROC and VLS configurations of the DD963 at four frequencies; 1.85, 6.34, 9.25, and 20.075 MHz. The VLS databases were cross-correlated with the ASROC databases to determine the magnitude of the complex cross-correlation coefficient, derive a bearing estimate, and compute bearing error. These data were then used to generate several displays which permitted the results to be interpreted.

3.1 Cross-correlation Surfaces

Figs. 8a and 8b show the numerical and experimental surfaces of cross-correlation for 1.85 MHz. The vertical (z) axis is the magnitude of the complex correlation coefficient ($0 \le |R| \le 1$), the horizontal (x) axis is the difference between the azimuth angle, ϕ, of the VLS signal and the azimuth angle, ϕ_t, of the ASROC database signal ($-180° \le (\phi - \phi_t) \le +180°$), and the axis receeding into the page (y axis) is the azimuth angle of arrival, ϕ, of the VLS signal ($0° \le \phi \le 360°$). If the DF system is performing properly, the surface will have low sidelobes, and a central ridge near $(\phi - \phi_t) = 0$ with $|R| \approx 1$. A configuration change which causes serious bearing errors will result in a surface with maximum correlation at other locations $(\phi - \phi_t) \neq 0$, usually with $|R| < 1$.

Although only 2D pictures can be presented here, in the actual simulation, the computer display of the cross-correlation surface is interactive and can be rotated about any axis to examine its properties. Figs. 8a and 8b show that simulation results using numerical and experimental DF antenna response data for the ASROC and VLS configurations agree quite well at 1.85 MHz.

3.2 Cross-correlation vs. Azimuth

A cut through the cross-correlation surface, perpendicular to the ϕ axis, yields a cross-correlation curve for a fixed signal angle of arrival, ϕ. A polar plot of this curve gives the relative response of the DF array vs. azimuth, in a format similar to that of a normal antenna pattern. Figs. 9a and 9b, show cuts through the numerical and experimental surfaces (Figs. 8a and 8b) for a signal arrival angle of 232 degrees, as indicated by the radial cursor. The numerical and experimental results both show peak correlation near 232 degrees, indicating little bearing error for this angle of arrival.

Again, only a static 2D result can be presented here, but in the actual simulation, the radial cursor, which indicates the angle of arrival on the computer display, can be moved to any azimuth using a mouse. As the cursor moves on the computer screen, the proper cross-correlation curve is displayed. Thus, a dynamic picture of the array response vs. azimuth can be quickly and easily obtained, and sectors where bearing errors occur can be easily identified.

3.3 Bearing Error vs. Azimuth

Figs. 10a and 10b show bearing error vs. azimuth at 1.85 MHz as determined from the simulation using numerical and experimental DF antenna responses. The curves both show a worst case bearing error of approximately ±2.5°. In particular, at 232°, both curves show a small negative bearing error. This negative error (bearing estimate less than true bearing) is also evident in Figs. 9a and 9b where the peak correlation can be seen to occur at a bearing slightly less than that of the cursor which indicates the true bearing.

The simulation can also be used to create a display of the 3 dimensional surface of bearing error vs. azimuth and frequency from curves of the type shown in Figs. 10. This surface makes it possible to easily identify areas of high bearing error over the entire domain of azimuth and frequency.

3.4 RMS Bearing Error

The last display which can be created using the simulation is one of RMS bearing error vs. frequency. In this display, the root mean square bearing error is computed over all azimuth angles at each frequency of interest. This provides an integrated measure of DF system performance. Table 1

Freq. (MHz)	1.85	6.34	9.25	20.077
Num.	1.11°	0.86°	2.80°	7.38°
Expt.	1.20°	0.39°	1.51°	6.20°

Table 1. RMS Bearing Error Predicted by the Simulation.

shows the results obtained using numerical and experimental DF antenna data at the four frequencies investigated in this study.

As indicated earlier, the accuracy of the numerical values of DF antenna response degraded with increasing frequency due to (most probably correctable) deficiencies in the wire

grid model of the DD963. This conclusion was reached by comparing numerical and experimental results and noting that the experimental antenna patterns appeared as one would expect based on frequency and location while the numerical patterns at the higher frequencies did not. That is, there is no reason to suspect that any of the experimental data is incorrect. Thus, simulation results (correlation, bearing error) based on numerical and experimental data were also less consistent at the higher frequencies. This was expected as the simulation output depended on the DF antenna data. However, the data in Table 1 shows that even with this degradation, the RMS bearing error results track quite well since this is a performance measure which is integrated over azimuth. One can therefore tenatively conclude that the computer simulation will correctly predict when bearing error will be caused by a topside change of configuration even at frequencies where there is considerable error in the computation of some DF antenna responses.

4. Conclusions

This paper has presented the results of a study to determine if computer simulation could be used to build a decision support system to determine when topside changes in configuration might require recalibration of a ship's CIDF based high frequency direction finding system. A computer simulation of the DF system was constructed, DF antenna responses required to create the system database were computed, and measurements were made for validation purposes.

The most critical aspect of this work was the use of NEC 4.1 to compute the DF antenna responses. Satisfying results were obtained at the lower frequencies, but computed antenna patterns became less accurate with increasing frequency. This appears to be due to ship numerical modeling deficiencies which are believed to be correctable. Thus, the approach seems quite promising.

The need for additional work on several enabling technologies quickly became clear during the course of this investigation. First, methods which have previously been used to create numerical models of complex structures are laborious and time consuming. For a computer simulation such as that described in this paper to be realistically implemented, it must be possible to create and modify numerical models quickly and easily. Ideally, one would like to go seamlessly from a ship CAD file to the input file for a CEM code. Presently, one must use software to mesh a structure of interest, fix the result manually, and then translate the output to obtain an input file for the CEM code. When the code is run, errors will likely occur and again, manual work will be required to fix these. More work is needed here.

Good pre-processors and post-processors for NEC (or any other code) are also needed. There is a need to be able to quickly and easily find wires and segments identified in CEM code error and warning messages and to eliminate the conditions causing the problems. Model visualization and file editing capabilities are being developed but have not reached the point where this is a straight forward task for a large file. Lastly, additional work is needed on post processor display capabilities. The processor used for this work, for example, did not permit display of receive antenna amplitude and phase data from the NEC output file, and it was therefore necessary to develop separate software for this purpose.

Lastly, difficulties were encountered using NEC to determine the receiving patterns of multiple antennas. For this, one needs the antenna feedpoint currents. To print only the 24 antenna feedpoint currents, it was necessary to place the feedpoint segments at the beginning of the file, so they appeared in sequence and the NEC print command (PT) could be used to obtain all 24 currents in one run. This required breaking up the input file which is undesirable. It would be much more desirable to be able to reuse the PT command to force printing of the current for each segment desired in a given run.

Acknowledgements

The work reported here represents a significant effort which could not have been accomplished without the support and participation of a number of individuals and organizations.

First and foremost, the author wishes to acknowledge the role of CAPT Charles Ristorcelli, Space and Naval Warfare Systems Command (SPAWAR), who had the foresight to recognize the potential of this research and to support it. John Lovegrove and Gary Wang, also of SPAWAR, helped, particularly in the early phases of the project. John Lovegrove organized a Ship Calibration Workshop which was held at the Naval Command Control and Ocean Surveillance Center RDT&E Division (NRaD) in San Diego in March 1994. Presentations and discussions included a review of previous modeling efforts and led to the decision to develop the computer simulation described in this paper. The wire grid numerical models of the DD963 were created for the author under subcontract with NRaD by Mr. Lance Koyama. At the Naval Postgraduate School (NPS), Prof. Beny Neta of the Mathematics Department assisted with the installation of NEC 4.1 on several platforms, including the School's CRAY J90, and parallelized the code to reduce run time (see Ref. [11]). Helpful discussions regarding the use of NEC in this application were held with Gerald Burke at Lawrence Livermore Laboratory, Dr. Jay Rockway at NRaD, and Prof. Dick Adler at NPS. A NEC processor, used primarily for visualization, was developed at NRaD by Linda Russell, and was ported, under subcontract to NRaD, to the Silicon Graphics workstation used in this project. Without the visualization capability provided by this software, it would have been extremely difficult, if not impossible to work with a structure as complex as the DD963. In the initial stages of the project, Dr. Ashok Das, under subcontract with Rolands & Associates, assisted with computer runs, developed MatLab programs to display the numerical and experimental DF antenna receive responses, and installed, debugged, and modified a number of programs required in the simulation. The DD 963 brass model measurement program conducted at NRaD was planned with the assistance of Mr. Bill Kordela, and was executed by Mr. Carl Firman. Invaluable assistance was also provided by Mr. Roy Overstreet, Naval In-Service Support Engineering (West), who was able to answer numerous important questions based on his experience with the DF system, and also provided a number of the system software programs which were used in the simulation. The graphic display programs essential to the interpretation of simulation results were developed by LT Steve Robey, USN, for his MSEE thesis. Lastly, support was also provided by the Naval Postgraduate School Direct Funded Research Program which provided funds for cost sharing with the sponsor on this project. The project described in this paper could not have been carried to a successful conclusion without the contributions of these individuals and organizations.

References

[1] A. Price, ***The History of US Electronic Warfare.*** Alexandria, VA: Association of Old Crows, 1984, Ch. 3, pp.35-36, Ch. 5, pp. 68.

[2] P. G. Redgment, "High frequency direction finding in the Royal Navy - Development of equipment for use against U-boats, Part 1", ***Journal of Naval Science***, Vol. 8, No. 1, pp. 32-43, 1982.

[3] P. G. Redgment, "High frequency direction finding in the Royal Navy - Development of equipment for use against U-boats, Part 2", ***Journal of Naval Science***, Vol. 8, No. 2, pp. 93-103, 1982.

[4] C. Crampton, et al., "The performance of high-frequency direction-finders in various types of H.M. ships", ***Journal of the Institution of Electrical Engineers***, Vol. 94:3A, Part No. 15, pp. 798-814, 1947.

[5] D. N. Travers, et al., "Multiloop antenna arrays for high-frequency shipboard direction finding", ***IEEE Trans. Ant. and Prop.***, Vol. AP-13, pp. 665-671, 1965.

[6] N. Saucier and K. Struckman, "Direction finding using correlation techniques," ***Proc. IEEE Intnl. Symp. on Antennas and Propagation***, pp. 260-263, June 1975.

[7] G. J. Burke, "Numerical Electromagnetics Code - NEC-4 Method of Moments, Part I: User's Manual", Report UCRL-MA-109338, Lawrence Livermore National Laboratory, Livermore, CA, January 1992.

[8] W. Johnson, et al., "Patch Code Users' Manual", Report SAN87-2991, Sandia National Laboratories, Alburquerque, NM, May 1988.

[9] J. B. Knorr and D. C. Jenn, "A numerical and experimental investigation of a semi-loop antenna on a metal box," ***Proc. 12th Annual Review of Progress in Applied Computational Electromagnetics***, Monterey, CA, pp. 832-839, March 18-22, 1996.

[10] J. B. Knorr, "A numerical and experimental investigation of a shipboard DF antenna array," ***Proc. 12th Annual Review of Progress in Applied Computational Electromagnetics***," Monterey, CA, pp. 792-801, March 18-22, 1996.

[11] B. Neta and J. B. Knorr, "Running NEC4 on the Cray at NPS," ***Applied Computational Electromagnetics Society Newsletter***, Vol. 11, No. 3, pp. 12-15, November 1996.

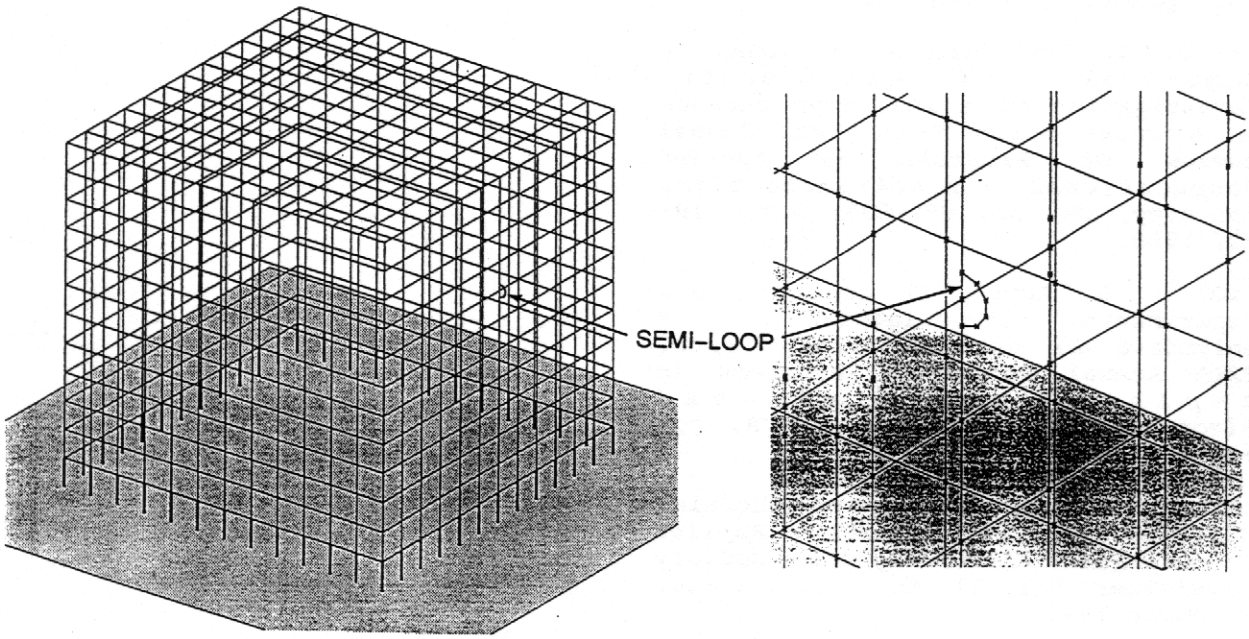

Figure 1. NEC model of the semi-loop antenna on a metal cube.

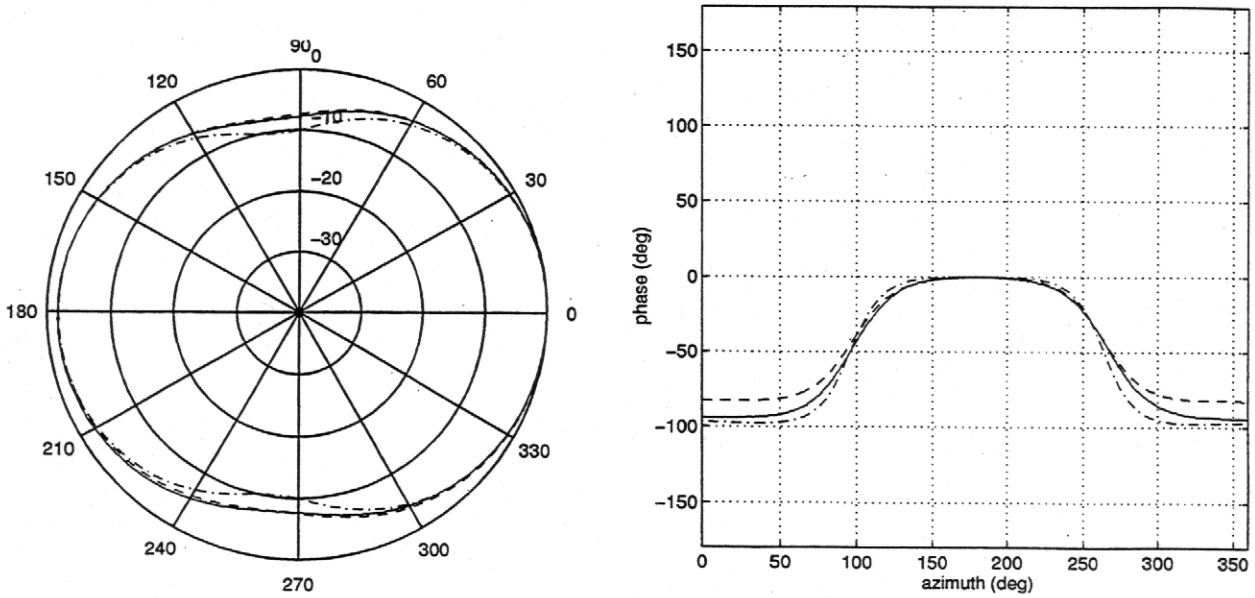

Figure 2. Numerical and experimental amplitude and phase responses for semi-loop antenna on a metal box. Frequency is 96 MHz (2 MHz scaled X48). (___ = measured, -- = PATCH, _._. = NEC)

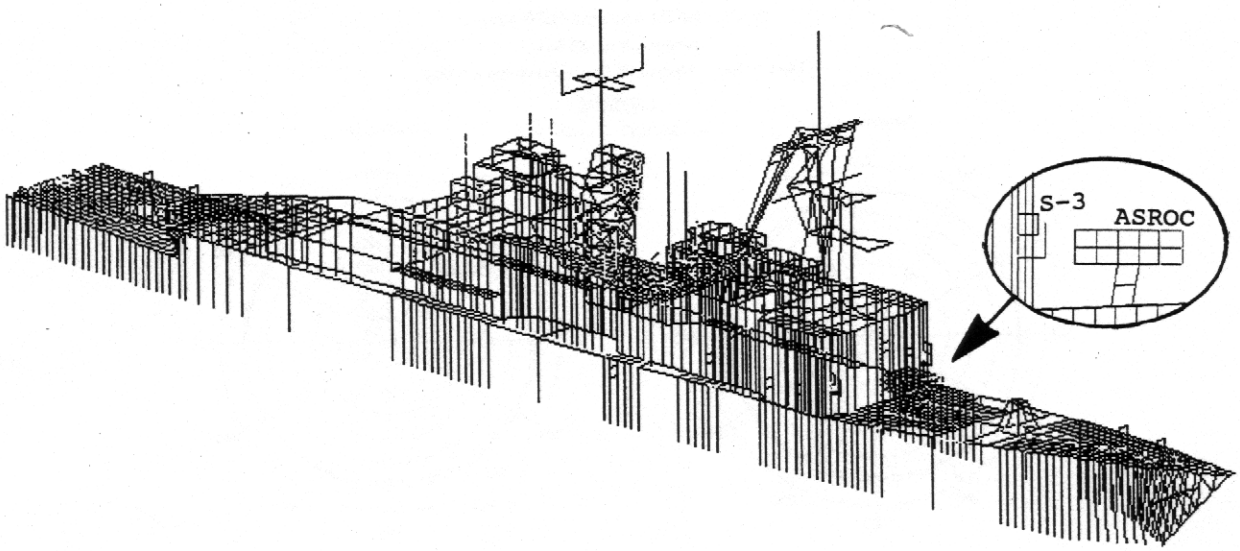

Figure 3a. Visualization of numerical model of DD963 in ASROC configuration.

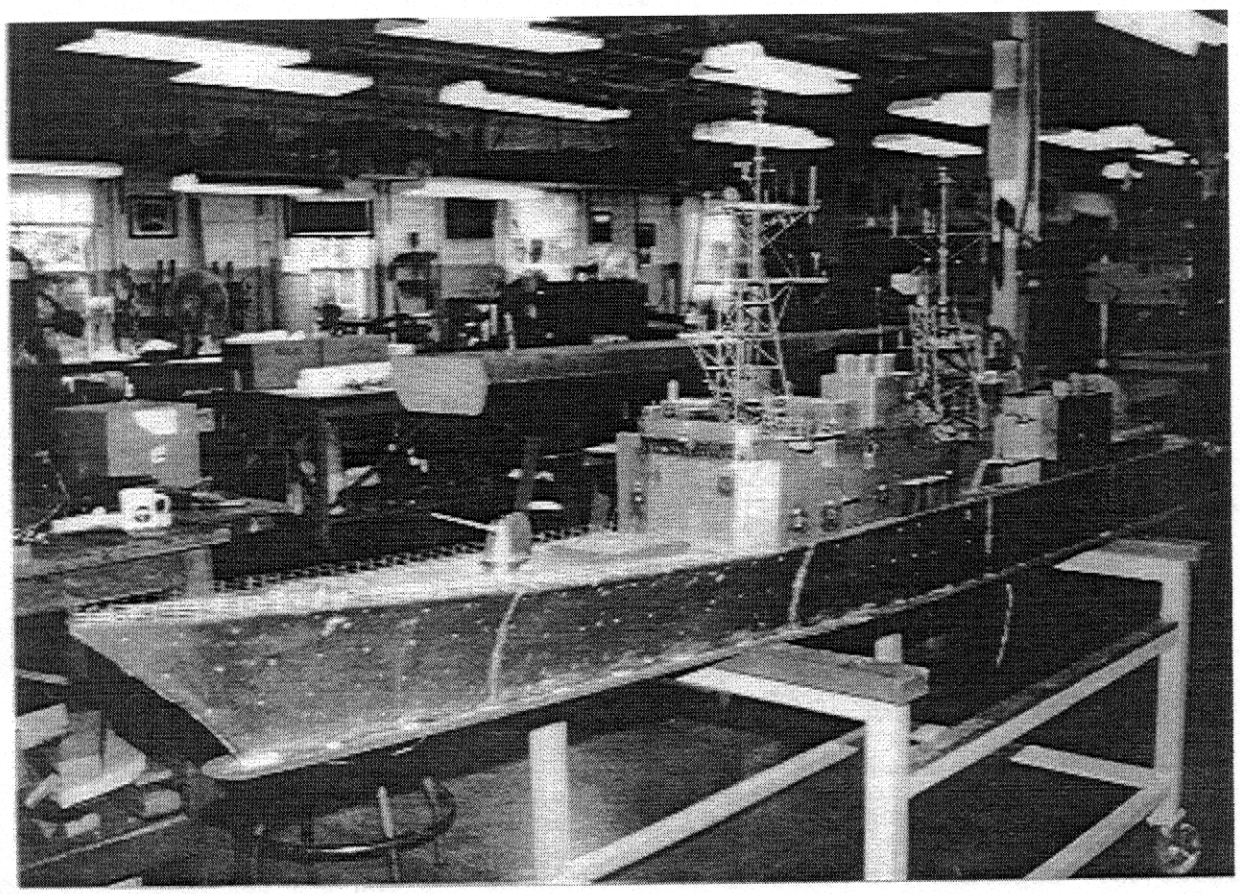

Figure 3b. Brass (experimental) model of DD963 in VLS configuration.

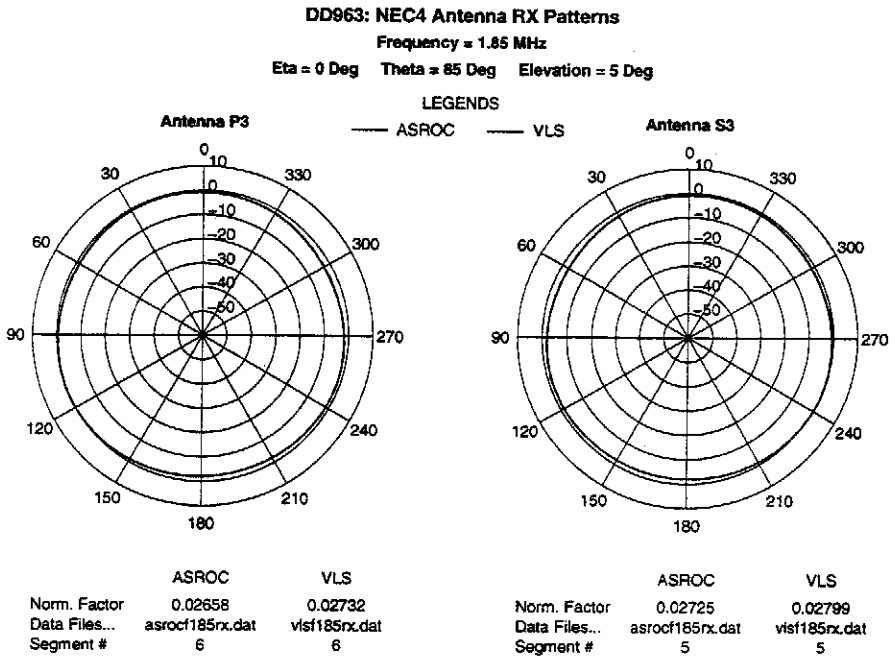

Figure 4a. Numerical patterns of DF antennas P-3 and S-3 for ASROC and VLS configurations of DD963. Elevation angle is 5 degrees, frequency is 1.85 MHz.

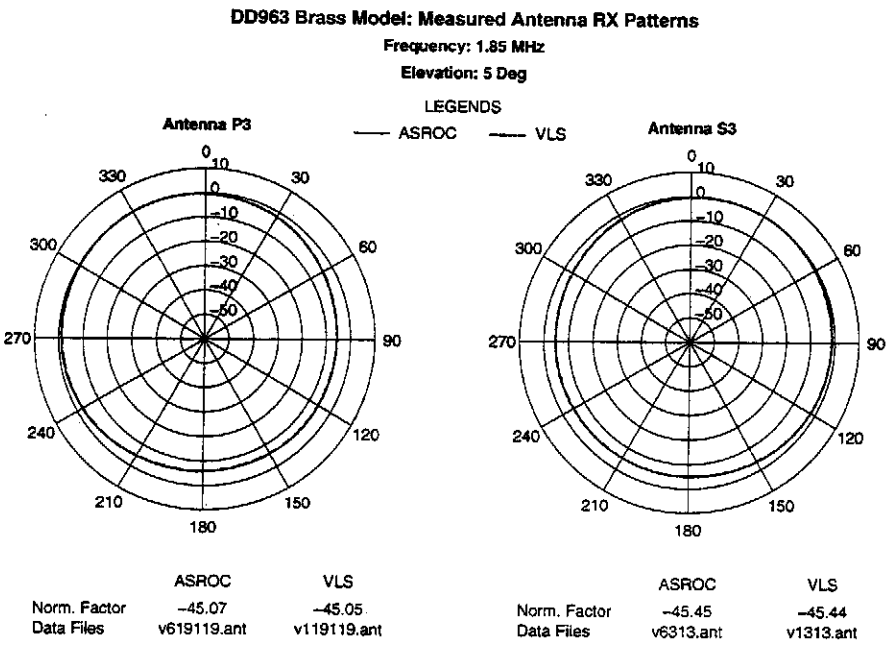

Figure 4b. Experimental patterns of DF antennas P-3 and S-3 for ASROC and VLS configurations of DD963. Elevation angle is 5 degrees, scaled frequency is 1.85 MHz.

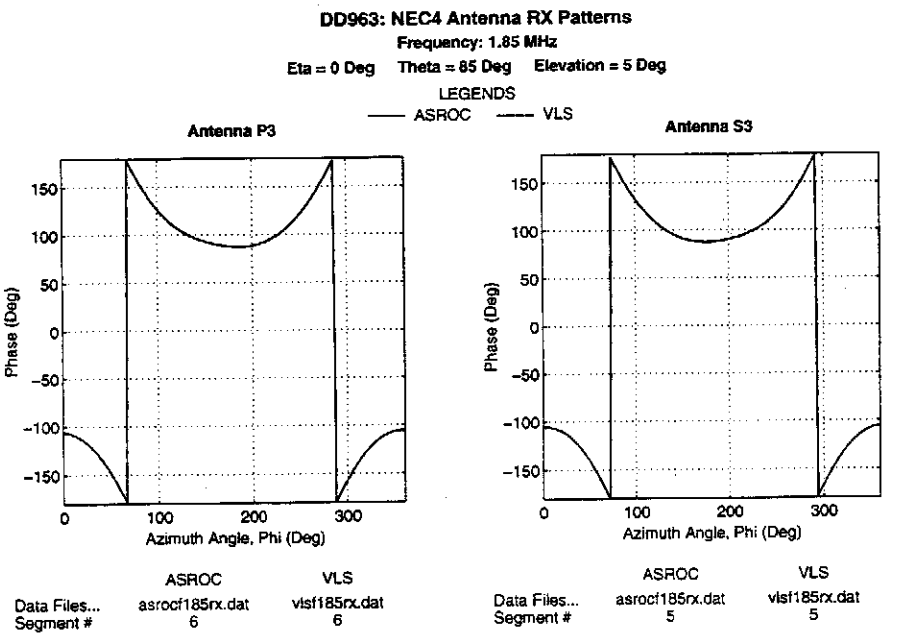

Figure 5a. Numerical phase of DF antennas P-3 and S-3 for ASROC and VLS configurations of DD963. Elevation angle is 5 degrees, frequency is 1.85 MHz.

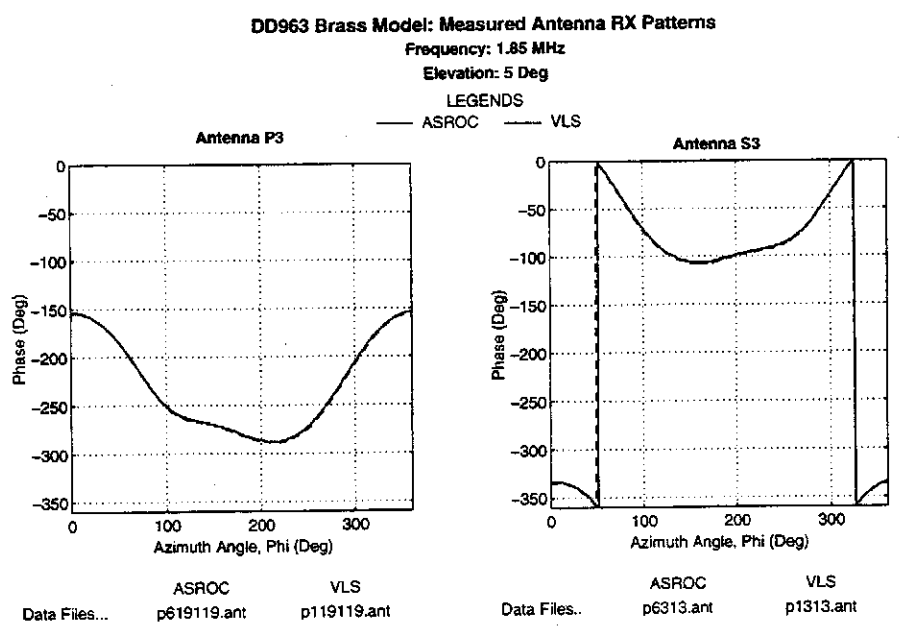

Figure 5b. Experimental phase of antennas P-3 and S-3 for ASROC and VLS configurations of DD963. Elevation angle is 5 degrees, scaled frequency is 1.85 MHz.

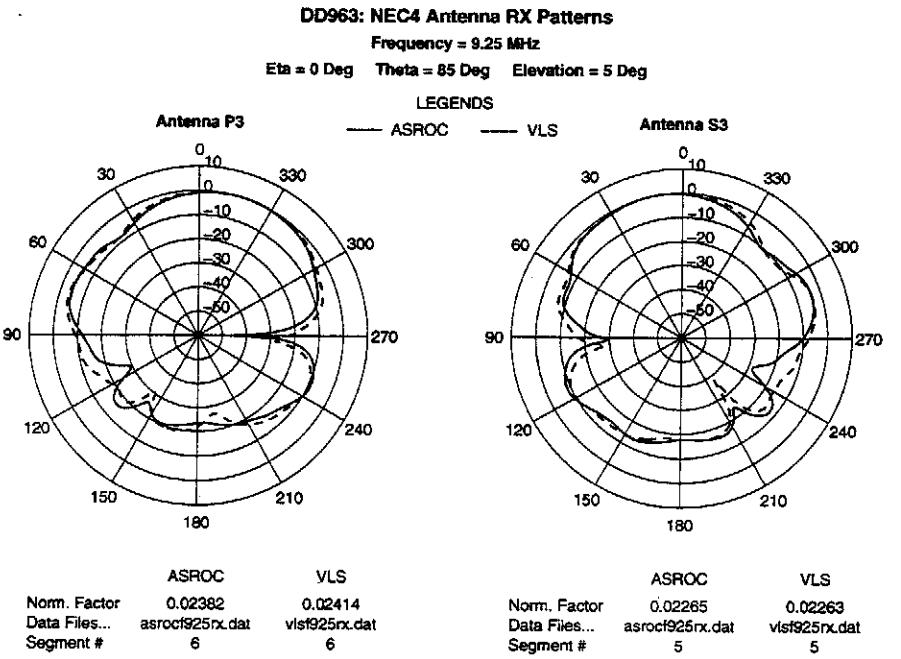

Figure 6a. Numerical patterns of antennas P-3 and S-3 for ASROC and VLS configurations of DD963. Elevation angle is 5 degrees, frequency is 9.25 MHz.

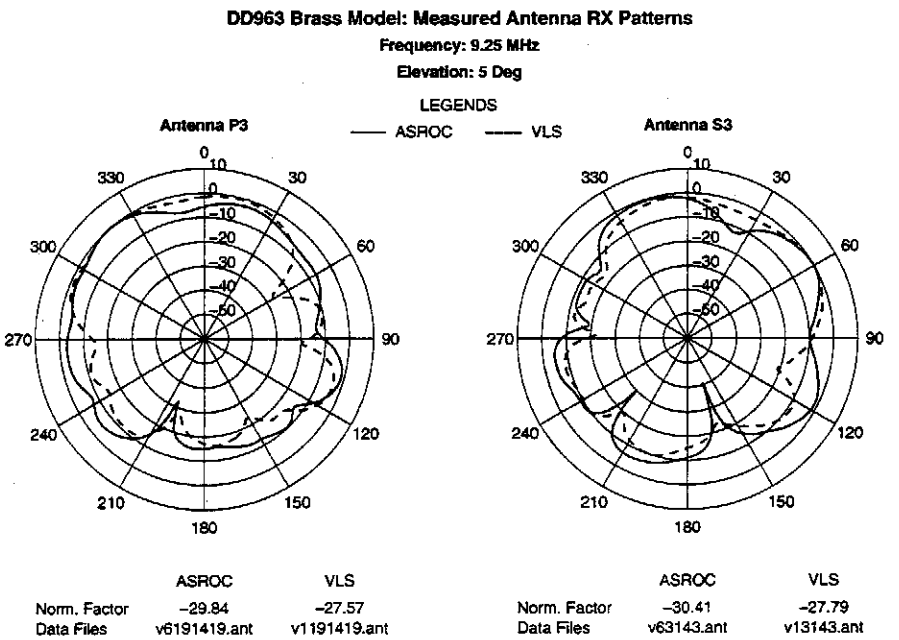

Figure 6b. Experimental patterns of antennas P-3 and S-3 for ASROC and VLS configurations of DD963. Elevation angle is 5 degrees, scaled frequency is 9.25 MHz.

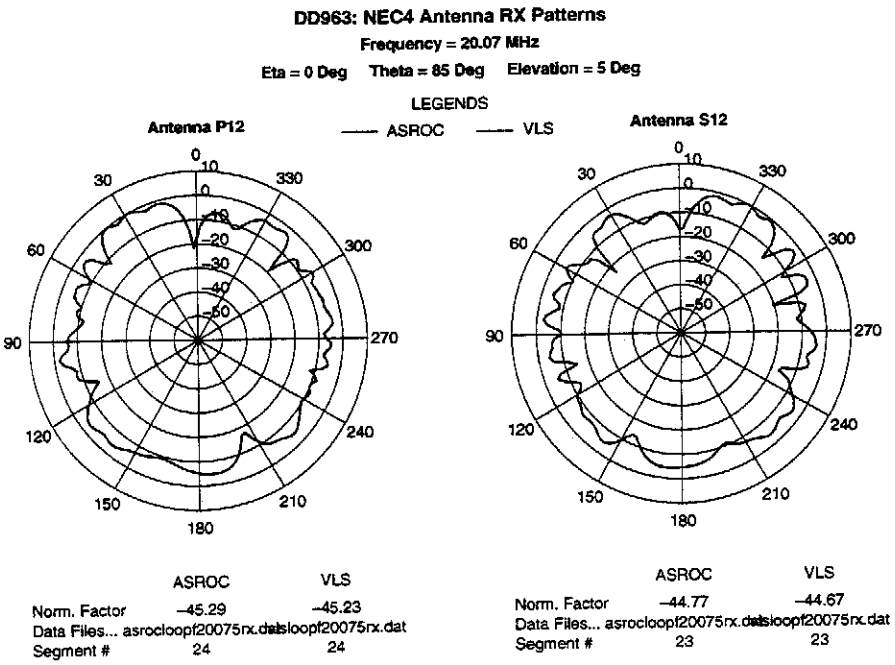

Figure 7a. Numerical patterns of DF antennas P-12 and S-12 for ASROC and VLS configurations of DD963. Elevation angle is 5 degrees, frequency is 20.075 MHz.

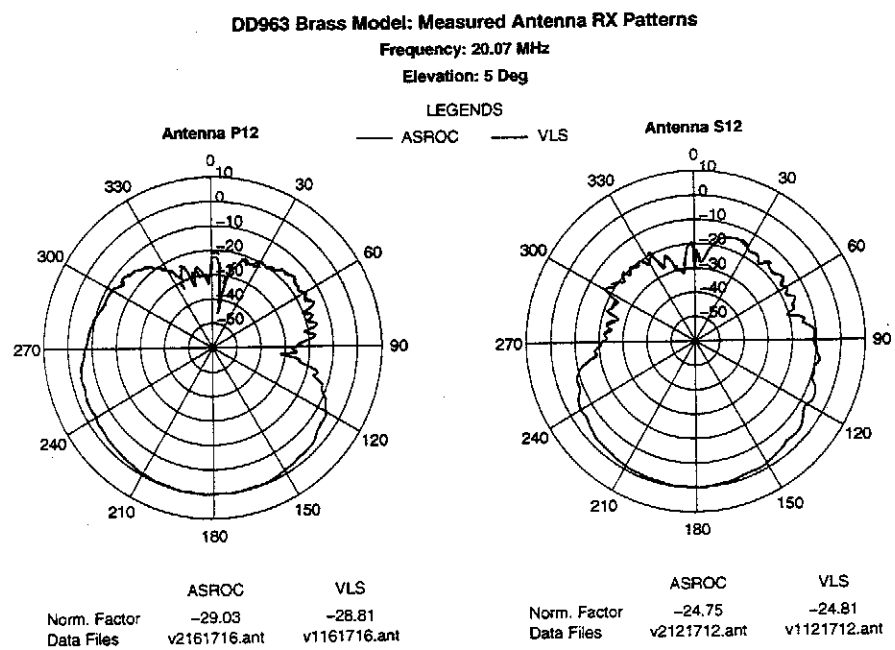

Figure 7b. Experimental patterns for DF antennas P-12 and S-12 for ASROC and VLS configurations of DD963. Elevation angle is 5 degrees, scaled frequency is 20.075 MHz.

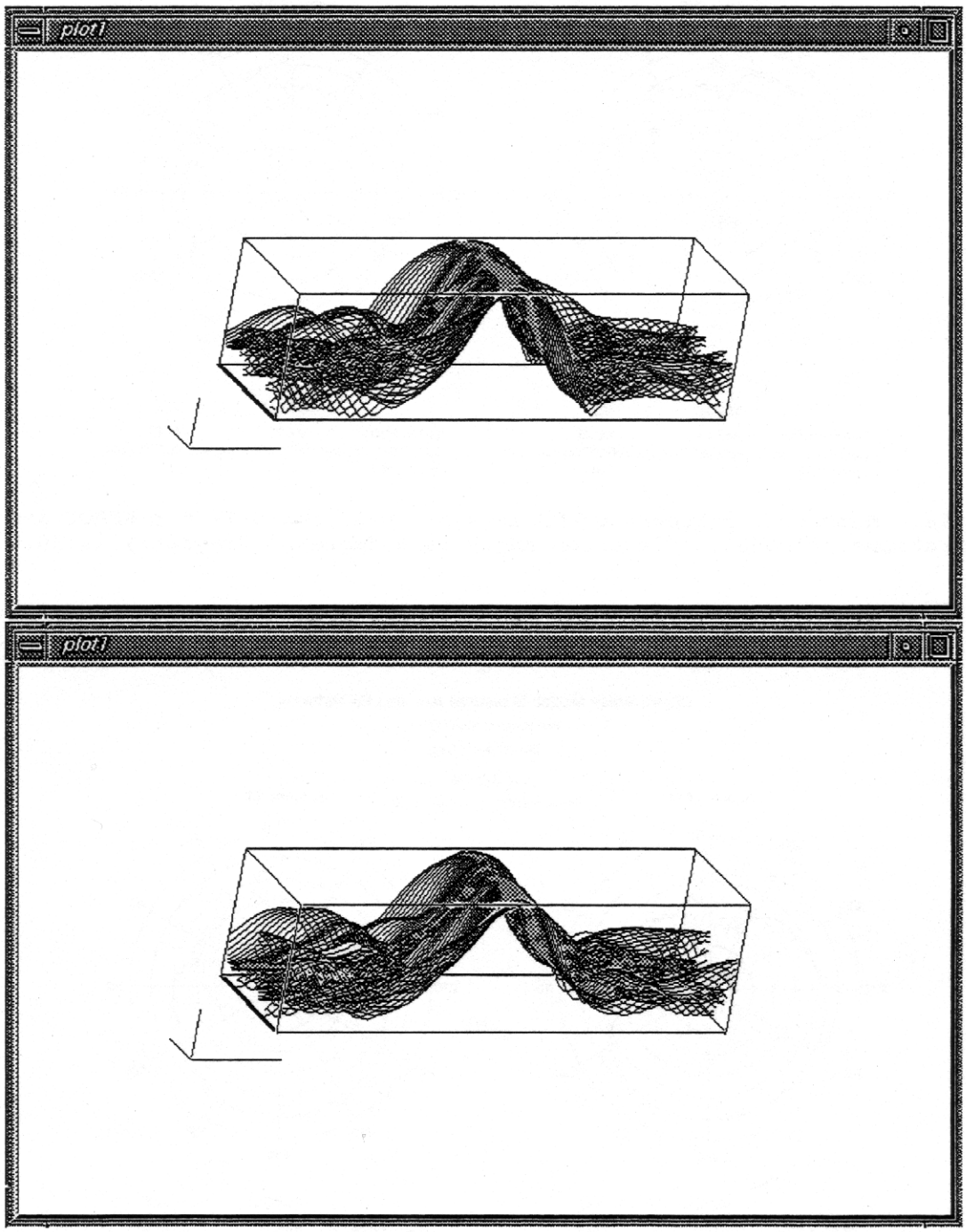

Figure 8. Cross-correlation surface, VLS vs. ASROC configuration of DD963. (a) Numerical result (top), 1.85 MHz, (b) Experimental result (bottom), 1.85 MHz scaled.

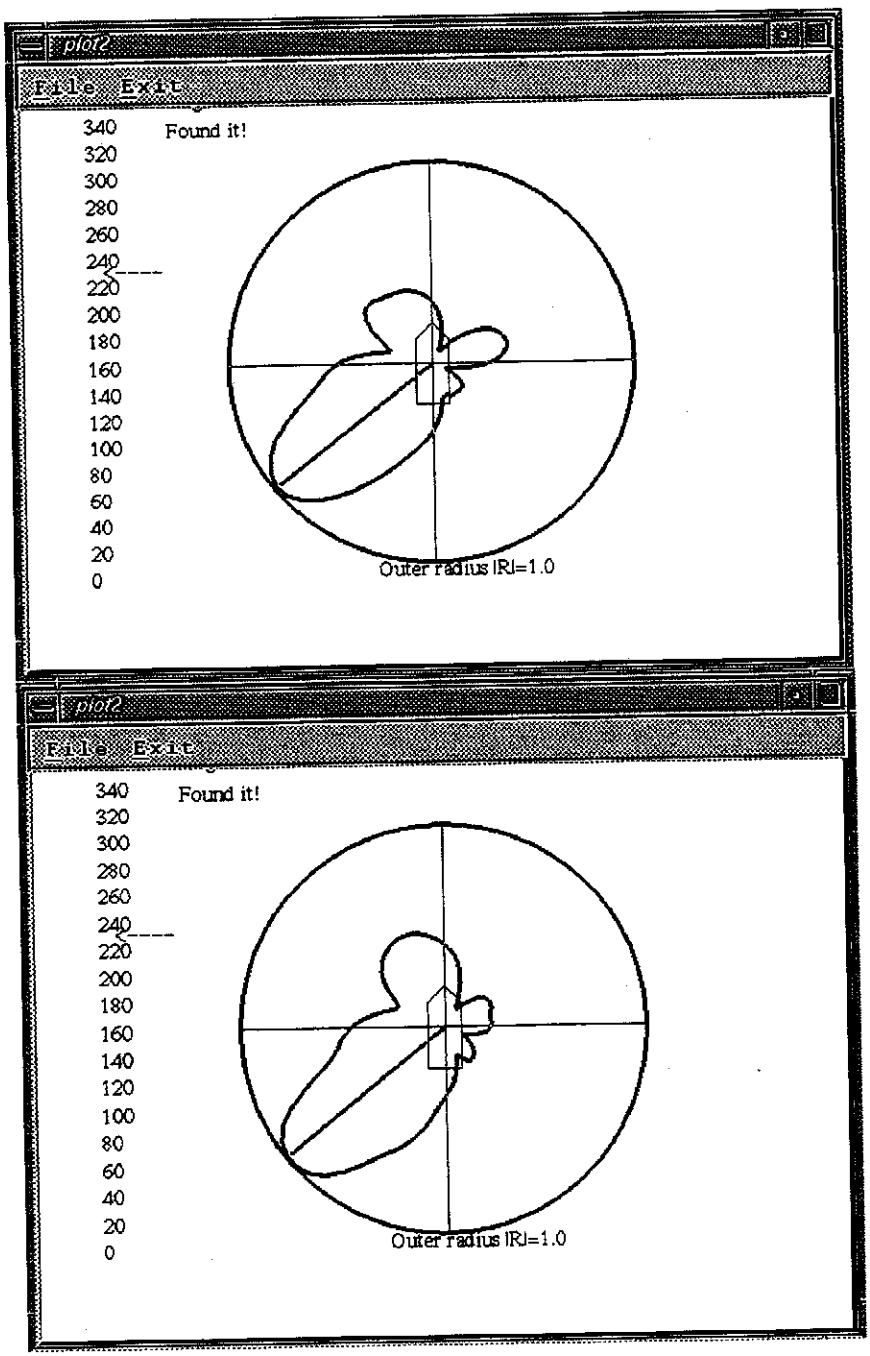

Figure 9. Cross-correlation vs. azimuth, VLS vs. ASROC configuration of DD963. Signal arrival angle is 232 degrees (indicated by cursor). (a) Numerical result (top), 1.85 MHz, (b) Experimental result (bottom), 1.85 MHz scaled.

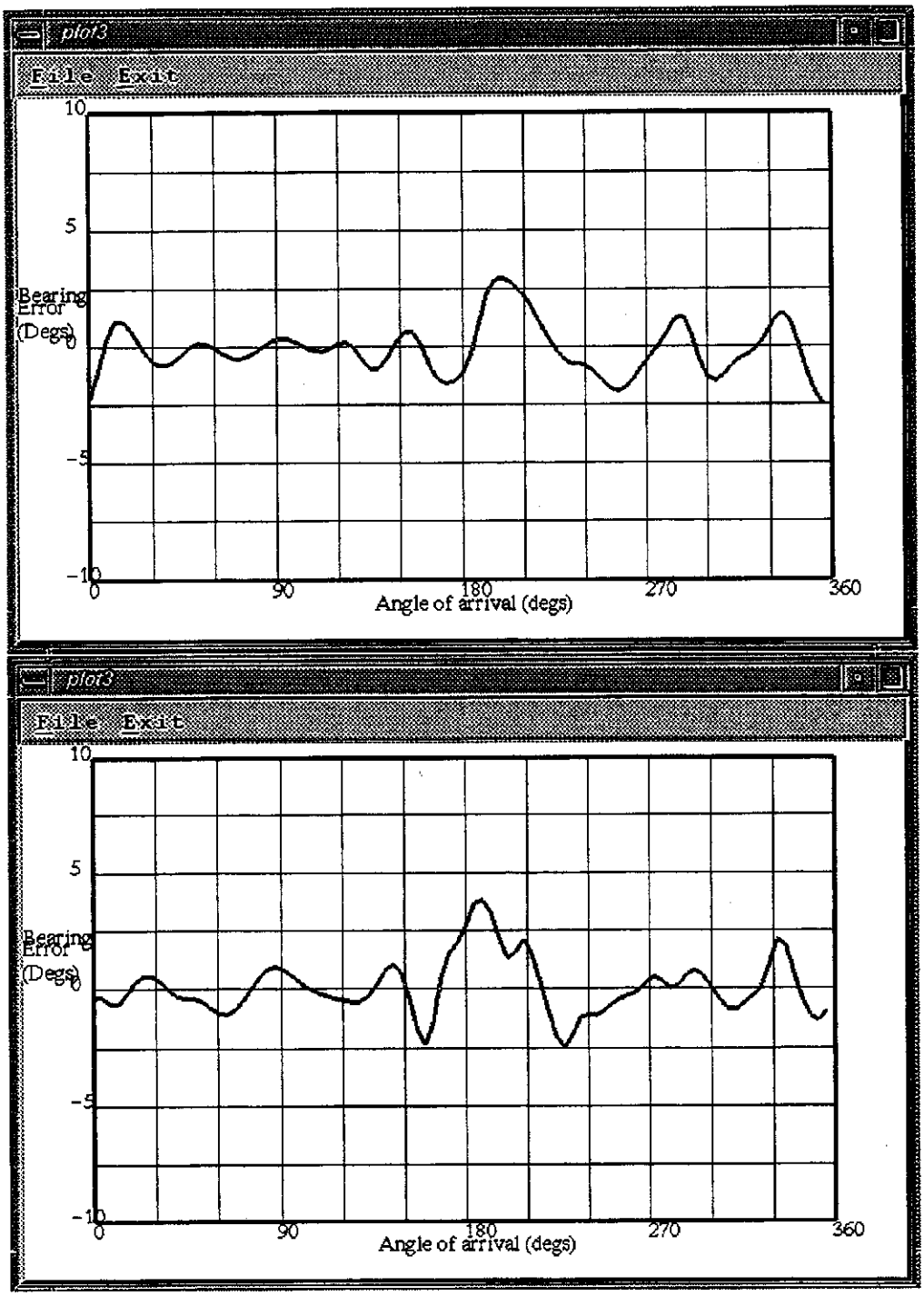

Figure 10. Bearing error vs. azimuth, VLS vs. ASROC configuration of DD963. (a) Numerical result (top), 1.85 MHz, (b) Experimental result (bottom), 1.85 MHz scaled.